*Article*

# Day-Ahead Scheduling of Multi-Energy Microgrids Based on a Stochastic Multi-Objective Optimization Model

**Seyed Reza Seyednouri** [1], **Amin Safari** [1], **Meisam Farrokhifar** [2,*], **Sajad Najafi Ravadanegh** [1], **Anas Quteishat** [3,4] **and Mahmoud Younis** [4]

1 Department of Electrical Engineering, Azarbaijan Shahid Madani University, Tabriz 5375171379, Iran
2 Department of the Built Environment, Eindhoven University of Technology, P.O. Box 513, 5600 MB Eindhoven, The Netherlands
3 Electrical Engineering Department, Faculty of Engineering Technology, Al Balqa Applied University, Al-Salt 19117, Jordan
4 Department of Electrical and Computer Engineering, Sohar University, P.O. Box 44, Sohar 311, Oman
* Correspondence: me.farrokhifar@gmail.com

**Abstract:** Dealing with multi-objective problems has several interesting benefits, one of which is that it supplies the decision-maker with complete information regarding the Pareto front, as well as a clear overview of the various trade-offs that are involved in the problem. The selection of such a representative set is, in and of itself, a multi-objective problem that must take into consideration the number of choices to show the uniformity of the representation and/or the coverage of the representation in order to ensure the quality of the solution. In this study, day-ahead scheduling has been transformed into a multi-objective optimization problem due to the inclusion of objectives, such as the operating cost of multi-energy multi-microgrids (MMGs) and the profit of the Distribution Company (DISCO). The purpose of the proposed system is to determine the best day-ahead operation of a combined heat and power (CHP) unit, gas boiler, energy storage, and demand response program, as well as the transaction of electricity and natural gas (NG). Electricity and gas are traded by MGs with DISCO at prices that are dynamic and fixed, respectively. Through scenario generation and probability density functions, the uncertainties of wind speed, solar irradiation, electrical, and heat demands have been considered. By using mixed-integer linear programming (MILP) for scenario reduction, the high number of generated scenarios has been significantly reduced. The $\varepsilon$-constraint approach was used and solved as mixed-integer nonlinear programming (MINLP) to obtain a solution that meets the needs of both of these nonlinear objective functions.

**Keywords:** energy hub; stochastic day-ahead operation; multi-microgrid; energy storages; Pareto front

## 1. Introduction

### 1.1. Motivation

With limited sources of fossil fuels, renewable energy sources (RESs) are getting more attention. RESs suffer from uncertainties and a non-dispatchable nature due to their dependence on weather conditions [1,2]. Energy storage applications in energy systems can provide technical and economic benefits, as well as mitigate the intermittent nature of RESs [3]. MMGs have been introduced recently to interact with each other [4], which can be beneficial for both utilities and consumers, as they can share their energy resources to improve reliability and reduce cost [5,6]. Increasing the number of MGs in the MMG system contributes to scheduling challenges for MGs due to the existence of several components and uncertainties [7]. Approximately half of the energy demanded is for heating around the globe [8], so investigating MGs as multi-carrier systems is highly important. Due to the low price, low emissions, and high reliability and efficiency of NG, gas to power facilities can be a good solution for power shortages [9].

*1.2. Literature Review*

Robust optimization is one of the ways to consider the uncertainty of the system without needing a probability density function (PDF). The authors in [10] have implemented robust optimization (RO) to address the uncertainties of RES and load. The authors also used RO for the day-ahead operation of a MMG in grid-connected mode while accounting for RES and load uncertainties [11]. Stochastic optimization (SO), on the other hand, uses PDFs of uncertain parameters to generate scenarios and solve the scheduling problem to obtain an optimal solution [12]. In [13], SO is used to address the uncertainties of the RES, load, and grid price of networked multi-carrier microgrids considering water–energy nexus issues. The uncertainties of WT, PV, demand, and electricity price have been addressed in SO, and the problem of sizing RES and battery energy storage has been modeled as a MILP problem [14]. Ref. [5] used two-stage stochastic optimization to address the uncertainties of load and RES. Stochastic planning, along with the MILP method and a security-constrained joint expansion planning problem, was solved for an integrated power and NG system in [15]. RO is appropriate when overly conservative control actions are required and only a limited amount of information is available, whereas SO is used to avoid overly conservative control [16,17]. In this paper, the SO will be implemented to address the validity of uncertain parameters, using corresponding PDFs. Two methods of dealing with multi-objective optimization that do not require complicated mathematical equations are scalarization and Pareto. In the scalarization method, the multi-objective problem is converted into a single-objective problem using weights. Meanwhile, non-dominated solutions are obtained and displayed as a Pareto optimality front in the Pareto method [18].

Uncertain parameters related to growing RESs in power systems present distinct issues in optimal system operation, necessitating the expansion of flexible resources to maintain appropriate reliability levels [15]. Taking into account the advantages of gas-fired generators over conventional generation units, NG will supply 25% of the electric power generation in the world by 2050 [19]. The establishment of the NG network has also increased the popularity of CHP units in multi-carrier MMGs to produce heat and power simultaneously [20,21]. The optimal configuration of an off-grid multi-energy microgrid, considering the uncertainties of RES and load, was performed in [22], using a non-dominated, sorting, genetic algorithm to obtain a Pareto solution.

The optimal multi-objective energy scheduling of an MG in the presence of RESs to reduce cost and emissions was investigated in [23], using improved multi-objective differential evolutionary. Improved differential evolutionary was also used to deal with the multi-objective feature of the problem and finally calculate the Pareto front for cost and emission objectives. In [24], an energy optimization model was developed, utilizing a multi-objective genetic algorithm and multi-objective wind-driven optimization, with Pareto fronts using the non-linear sorting fuzzy mechanism to solve the multi-objective energy optimization problem, considering the uncertainties of solar and wind. The authors in [25] considered the uncertainties of electrical grid price, electrical and thermal demand, and solar irradiance, using scenario-based optimization in a multi-energy MG, with the goal of reducing the cost and emissions. The augmented $\varepsilon$-constraint method and MINLP programming were used to display the Pareto front, and the best compromise was chosen using fuzzy decision making. However, the presence of WT, microgrid interactions as MMG, and the entity of DISCO were not investigated in this paper. The authors in [26] investigated a stochastic day-ahead schedule of an MG with economic and emission improvement targets, using Pareto front and $\varepsilon$-constraint methods.

Energy storage systems (ESSs) are recognized as a countermeasure against the intermittent nature of RES in multi-energy systems [2]. The energy storage optimization of a multi-energy MG is proposed in [27] to reduce the cost and emissions. The authors in [28] studied the integration of battery energy storage with a CHP unit to increase the flexibility and reliability of the system and decrease operational costs.

### 1.3. Research Gap and Contributions

Although some research has been conducted on energy hubs and MMG, there is still a research gap for multi-energy MMG, where a cluster of MGs can schedule their energy carriers and resources in accordance with each other. Another research gap is the presence of DISCO in multi-energy systems, which facilitates the operation of MMGs and introduces practical challenges to energy systems through the procedure of trading energy with MGs and the grid. This paper investigates the stochastic day-ahead scheduling for a cluster of multi-energy MGs and a DISCO, where multiple uncertain parameters exist. The Pareto front and ε-constraint methods were used to solve the two conflicting objective functions because the MGs' cost reduction and DISCO's profit increase are optimized simultaneously. Electricity and NG are the energy carriers of this system, and consumers demand electricity and heat. Electricity prices for MGs are set dynamically, while gas prices are set to be fixed. The main contributions can be highlighted as follows:

- Considering the uncertainties of wind speed, solar irradiation, electric, and heat demand through scenario-based stochastic optimization.
- Presenting electric and heat energy storage, as well as electric DR, in the system structure and analyzing their effect on multi-energy MMG system operation and the dynamic price of electricity.
- Solving the MINLP stochastic problem through the ε-constraint method to obtain the Pareto front of the DISCO and MGs objectives and find the best compromise using a fuzzy decision-making approach.

### 1.4. Paper Organization

The rest of the paper is organized as follows. Section 2 describes the system model and mathematical formulation of DISCO and MGs objective functions and their components. Section 3 gives the simulated system data and its simulation results, along with a brief description of the results. Section 4 presents the conclusion of the paper, and following is the nomenclature.

## 2. Problem Formulation

### 2.1. System Description

This paper proposes a stochastic optimization framework for the optimal day-ahead schedule of an energy hub with a DISCO and an MMG. A detailed illustration of the proposed system can be seen in Figure 1. DISCO, as a dependent entity and as the first objective function, can exchange power and import NG from the grid. MG, as a dependent entity and as the second objective function, can exchange power and import NG from DISCO. The price of traded electric power between the grid and DISCO is based on the time of use, while the price of traded electric power between DISCO and MGs is dynamic and obtained during optimization. NG is traded at a fixed price between the grid and DISCO, as well as between DISCO and MGs. Each MG has WT, PV, CHP, and GB as energy resources and HS and BS as energy storage. CHP produces electricity and heat simultaneously, and GB produces heat, both of which consume NG. The consumers located in MGs demand both electricity and heat. A portion of the electric demand can participate in shiftable demand response.

### 2.2. Uncertainty Formulation

Wind speed, solar irradiation, electric, and heat demand uncertainty are all considered by generating their corresponding PDFs. The uncertainty of wind speed follows the Weibull distribution, which can be obtained using (1)–(3).
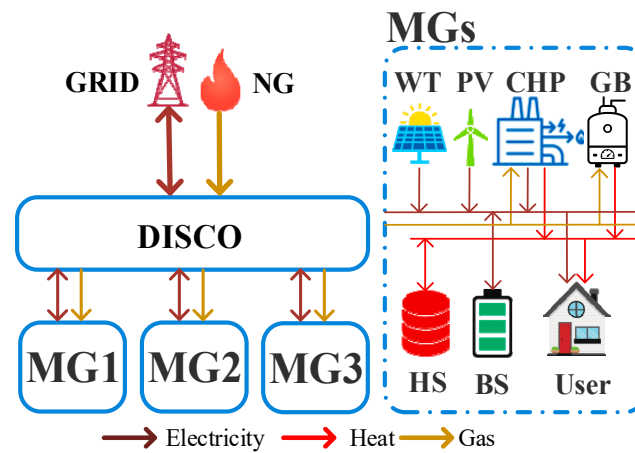
**Figure 1.** The structure of the proposed system.

$$PDF(v) = \frac{k}{c}\left(\frac{v}{c}\right)^{k-1} \exp\left(-\left(\frac{v}{c}\right)^{k}\right) \tag{1}$$

$$k = \left(\frac{\delta}{\mu}\right)^{-1.086} \tag{2}$$

$$c = \frac{\mu}{\Gamma\left(1 + \frac{1}{k}\right)} \tag{3}$$

The uncertainty of solar irradiation follows Beta distribution, which can be obtained using (4)–(6).

$$PDF(x) = \frac{\Gamma(\alpha + \beta)}{\Gamma(\alpha)\Gamma(\beta)} x^{\alpha-1} (1 - x)^{\beta-1} \tag{4}$$

$$\beta = (1 - \mu)\left(\frac{\mu(1 - \mu)}{\delta^2} - 1\right) \tag{5}$$

$$\alpha = \frac{\mu\beta}{1 - \mu} \tag{6}$$

The uncertainty of electric and heat demand follows the Normal distribution, which can be obtained using (7).

$$PDF\left(P^{demand}\right) = \frac{1}{\delta\sqrt{2\pi}} e^{-\frac{(P^{demand} - \mu)^2}{2\delta^2}} \tag{7}$$

Generating scenarios using the mentioned approaches will result in a higher number of scenarios, which can result in complexity in the optimization process. By using scenario reduction, the main scenarios can be reduced to a smaller number, while maintaining the same probable behavior as the initial set. The MILP scenario reduction is suggested for implementation, and its objective function is to find the minimum number of scenarios that maintain the characteristics of the initial scenarios. A full explanation can be found in [29,30].

### 2.3. DISCO-Level Formulation

The goal of this level is to maximize the profit of DISCO in day-ahead energy management by adjusting the amount of electricity and NG transacted between the grid and MGs

and the price of transactive electric energy. The objective function of this goal is formulated in (8).

$$OF_1 = \max \sum_t \sum_i \sum_s \rho_{t,s} \left( \pi^E_{t,i,s} P^E_{t,i,s} + \pi^G P^G_{t,i,s} - \pi^{Grid}_t P^{Grid}_{t,s} - \pi^{Gas} P^{Gas}_{t,s} \right) \tag{8}$$

Subjected to:

The upper and lower limits for traded electricity and NG between DISCO and the grid are shown in (9) and (10), respectively. In addition, the maximum and minimum levels of transactive electric energy are shown in (11). Constraints (12) and (13) ensure that the amount of MGs' electricity and gas demand is equal to the imported electricity and gas from the grid by DISCO.

$$-P^{Grid}_{\max} \leq P^{Grid}_{t,s} \leq P^{Grid}_{\max}, \quad \forall t, s \tag{9}$$

$$0 \leq P^{Gas}_{t,s} \leq P^{Gas}_{\max}, \quad \forall t, s \tag{10}$$

$$\pi^E_{i,\min} \leq \pi^E_{t,i,s} \leq \pi^E_{i,\max}, \quad \forall t, i, s \tag{11}$$

$$\sum_i P^E_{t,i,s} = P^{Grid}_{t,s}, \quad \forall t, i, s \tag{12}$$

$$\sum_i P^G_{t,i,s} = P^{Gas}_{t,s}, \quad \forall t, i, s \tag{13}$$

*2.4. MG-Level Formulation*

The objective of MGs is to reduce their operation and generation costs through optimal energy trade with DISCO and the operation schedule of its components, which is shown in (14). The first and second terms stand for the cost of purchasing electricity and natural gas from wholesale markets, respectively. The third term stands for the cost of the DR program, and the last term specifies the cost of energy not supply (ENS) for consumers.

$$OF_2 = \min \sum_t \sum_i \sum_s \rho_{t,s} \left( \pi^E_{t,i,s} P^E_{t,i,s} + \pi^G P^G_{t,i,s} + \pi^{DR}(P^{DRU}_{t,i} + P^{DRD}_{t,i}) + \pi^{ENS} P^{ENS}_{t,i,s} \right) \tag{14}$$

Subjected to:

The electricity that is exchanged and the NG that is brought in from DISCO are limited by (15) and (16), respectively.

$$-P^E_{i,\max} \leq P^E_{t,i,s} \leq P^E_{i,\max}, \quad \forall t, i, s \tag{15}$$

$$0 \leq P^G_{t,i,s} \leq P^G_{i,\max}, \quad \forall t, i, s \tag{16}$$

2.4.1. WT

The equation for WT power generation is given in (17). The WT output is dependent on wind speed and can only generate power when the wind speed is between the cut-in and cut-out speeds of the WT.

$$P^{WT}_{t,i,s} = \begin{cases} 0 & v_{t,s} < V_{ci} \text{ or } v_{t,s} > V_{co} \\ P^{WT}_{i,r} \times \frac{v_{t,s} - V_{ci}}{v_r - V_{ci}} & V_{ci} \leq v_{t,s} < V_r \\ P^{WT}_{i,r} & V_r \leq v_{t,s} < V_{co} \end{cases} \tag{17}$$

### 2.4.2. PV

Another renewable resource in MG's structure is solar PV, which produces power from solar irradiation and whose output also depends on ambient temperature. The PV output power can be calculated using (18).

$$P_{t,i,s}^{PV} = P_{PV,i}^{STC} \frac{\Phi_{t,s}}{\Phi_i^{STC}} [1 + K(T_{a,t} - 25)] \tag{18}$$

### 2.4.3. CHP Units

A CHP unit consumes NG to generate heat and power simultaneously, and it has higher efficiency compared to that of single heat or power generation. Power and heat generation are calculated using (19) and (20). The amount of NG consumed by CHP units and its ram rate are limited by (21)–(23).

$$P_{t,i,s}^{e,CHP} = \eta_i^{e,CHP} P_{t,i,s}^{g,CHP}, \quad \forall t,i,s \tag{19}$$

$$P_{t,i,s}^{h,CHP} = \eta_i^{h,CHP} P_{t,i,s}^{g,CHP}, \quad \forall t,i,s \tag{20}$$

$$0 \le P_{t,i,s}^{g,CHP} \le P_{i,\max}^{g,CHP}, \quad \forall t,i,s \tag{21}$$

$$-P_i^{d,CHP} \le P_{t,i,s}^{g,CHP} - P_{t-1,i,s}^{g,CHP} \le P_i^{u,CHP}, \quad \forall t > 1, i, s \tag{22}$$

$$-P_i^{d,CHP} \le P_{t,i,s}^{g,CHP} - P_{i,ini}^{g,CHP} \le P_i^{u,CHP}, \quad \forall t = 1, i, s \tag{23}$$

### 2.4.4. Gas Boiler

A gas boiler produces heat by consuming NG. The produced heat and consumed NG limit are shown in (24) and (25), respectively.

$$P_{t,i,s}^{h,GB} = \eta_i^{GB} P_{t,i,s}^{g,GB}, \quad \forall t,i,s \tag{24}$$

$$0 \le P_{t,i,s}^{g,GB} \le P_{i,\max}^{g,GB}, \quad \forall t,i,s \tag{25}$$

### 2.4.5. Battery Storage

The amount of stored electric power in batteries is displayed in (26) and (27), which is also restricted by (28). Constraints (29) and (30) are for the charging and discharging rates of batteries, respectively. Constraint (31) prevents the battery from simultaneously charging and discharging, while constraint (32) assures that the amount of stored power at the beginning of the simulation period is identical to the stored power at the end of the simulation period.

$$SoC_{t,i,s}^{BS} = SoC_{t-1,i,s}^{BS} + \eta^{ch,BS} P_{t,i}^{ch,BS} - P_{t,i}^{dch,BS} / \eta^{dch,BS}, \quad \forall t > 1, i, s \tag{26}$$

$$SoC_{t,i,s}^{BS} = SoC_i^{ini,BS} + \eta^{ch,BS} P_{t,i}^{ch,BS} - P_{t,i}^{dch,BS} / \eta^{dch,BS}, \quad \forall t = 1, i, s \tag{27}$$

$$SoC_{i,\min}^{BS} \le SoC_{t,i,s}^{BS} \le SoC_{i,\max}^{BS}, \quad \forall t,i,s \tag{28}$$

$$0 \le P_{t,i}^{ch,BS} \le Z_{t,i}^{ch,BS} P_{i,\max}^{BS}, \quad \forall t,i \tag{29}$$

$$0 \le P_{t,i}^{dch,BS} \le Z_{t,i}^{dch,BS} P_{i,\max}^{BS}, \quad \forall t,i \tag{30}$$

$$Z_{t,i}^{ch,BS} + Z_{t,i}^{dch,BS} \le 1, \quad \forall t,i \tag{31}$$

$$SoC_{t=0,i,s}^{BS} = SoC_{t=T,i,s}^{BS}, \quad \forall t,i,s \tag{32}$$

### 2.4.6. Heat Storage

The amount of stored heat in heat storage is expressed in (33) and (34), which is restricted by the minimum and maximum amounts in (35). The charge and discharge rate of heat are shown in (36) and (37), respectively. Constraint (38) does not allow the simultaneous charge and discharge of heat, and constraint (39) assures that the amount of stored heat at the beginning of the simulation period is identical to the stored heat at the end of the simulation period.

$$SoC_{t,i,s}^{HS} = SoC_{t-1,i,s}^{HS} + \eta^{ch,HS} P_{t,i}^{ch,HS} - P_{t,i}^{dch,HS} / \eta^{dch,HS}, \quad \forall t > 1, i, s \tag{33}$$

$$SoC_{t,i,s}^{HS} = SoC_{i}^{ini,HS} + \eta^{ch,HS} P_{t,i}^{ch,HS} - P_{t,i}^{dch,HS} / \eta^{dch,HS}, \quad \forall t = 1, i, s \tag{34}$$

$$SoC_{i,\min}^{HS} \leq SoC_{t,i,s}^{HS} \leq SoC_{i,\max}^{HS}, \quad \forall t, i, s \tag{35}$$

$$0 \leq P_{t,i}^{ch,HS} \leq Z_{t,i}^{ch,HS} P_{i,\max}^{HS}, \quad \forall t, i \tag{36}$$

$$0 \leq P_{t,i}^{dch,HS} \leq Z_{t,i}^{dch,HS} P_{i,\max}^{HS}, \quad \forall t, i \tag{37}$$

$$Z_{t,i}^{ch,HS} + Z_{t,i}^{dch,HS} \leq 1, \quad \forall t, i \tag{38}$$

$$SoC_{t=0,i,s}^{HS} = SoC_{t=T,i,s}^{HS}, \quad \forall t, i, s \tag{39}$$

### 2.4.7. Demand Response

Shiftable demand response has been utilized to add flexibility to the electric part of the energy hub. Constraints (40) and (41) show the amount of electric power that can be delayed to a different time for economic reasons. According to (42), the sum of shift up load and the sum of shift down load must be equal. Simultaneous shift up and shift down in each time interval are prevented by using (43).

$$0 \leq P_{t,i}^{DRU} \leq Z_{t,i}^{DRU} P_{\max}^{DRU}, \ \forall t, i \tag{40}$$

$$0 \leq P_{t,i}^{DRD} \leq Z_{t,i}^{DRD} P_{\max}^{DRD}, \ \forall t, i \tag{41}$$

$$\sum_t P_{t,i}^{DRU} = \sum_t P_{t,i}^{DRD}, \ \forall t, i \tag{42}$$

$$Z_{t,i}^{DRU} + Z_{t,i}^{DRD} \leq 1, \ \forall t, i \tag{43}$$

### 2.4.8. Electric Power Balance

According to (44), the electric demand must be supplied using local energy resources, imported power from DISCO, and flexibilities introduced by a battery and DR.

$$P_{t,i,s}^{e,CHP} + P_{t,i,s}^{WT} + P_{t,i,s}^{PV} + P_{t,i}^{dch,BS} + P_{t,i,s}^{E} + P_{t,i,s}^{DRD} + P_{t,i,s}^{ENS} = P_{t,i,s}^{Edemand} + P_{t,i}^{ch,BS} + P_{t,i,s}^{DRU}, \ \forall t, i, s \tag{44}$$

### 2.4.9. Heat Power Balance

According to (45), the heat demand must be supplied with the generated heat of the CHP and GB units, with the help of heat energy storage.

$$P_{t,i,s}^{h,CHP} + P_{t,i,s}^{h,GB} + P_{t,i}^{dch,HS} = P_{t,i}^{Hdemand} + P_{t,i}^{ch,HS}, \ \forall t, i, s \tag{45}$$

### 2.4.10. Gas Balance

Constraint (46) states that the NG imported from DISCO should be identical to the NG consumed by the CHP and GB units.

$$P_{t,i,s}^{G} = P_{t,i,s}^{g,CHP} + P_{t,i,s}^{g,GB}, \quad \forall t, i, s \tag{46}$$

*2.5. Solution Methodology*

Maximizing DISCO profit and minimizing MGs are two conflicting objective functions. The Pareto front and $\varepsilon$-constraint methods were used to find a compromise between these objective functions [31,32]:

1.  Find the maximum and minimum values of $OF_2$ and save them.
2.  Add $OF_2$ to the constraints as follows:

$$OF_2 \geq \varepsilon \tag{47}$$

3.  The value of $\varepsilon$ varies between the minimum and maximum values $OF_2$, while $OF_1$ is maximized.

Finally, the best compromise was selected using fuzzy decision making. The membership value for the $n$th objective function of the $j$th solution in the Pareto front is found by the membership function defined in (48).

$$\mu_n^j = \begin{cases} 0 & OF_n \leq OF_n^{\min} \\ \frac{OF_n - OF_n^{\min}}{OF_n^{\max} - OF_n^{\min}} & OF_n^{\min} \leq OF_n < OF_n^{\max} \\ 1 & OF_n < OF_n^{\max} \end{cases} \tag{48}$$

The solution with the highest value of $\mu^j$, calculated using (49), is selected as the optimal solution.

$$\mu^j = \frac{\sum\limits_n W_n \mu_n^j}{\sum\limits_j \sum\limits_n W_n \mu_n^j} \tag{49}$$

The complete procedure of the proposed system optimization is summarized in the flow chart illustrated in Figure 2.
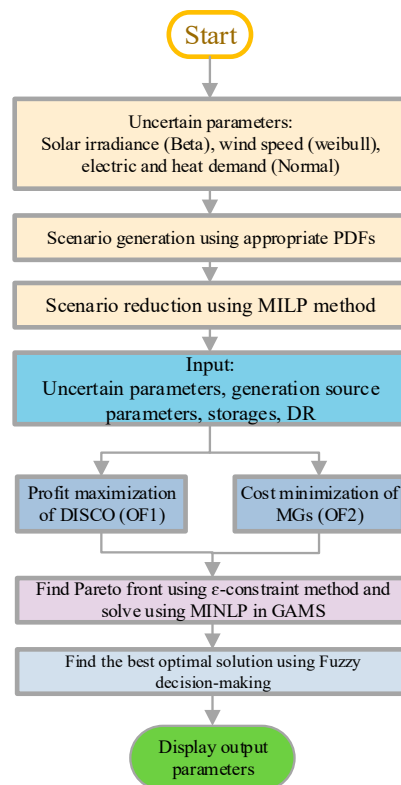


**Figure 2.** Solution steps for stochastic multi-objective optimization.

## 3. Simulation Results

### 3.1. System Data

The proposed system was investigated for a hypothetical distribution system, using GAMS and MATLAB software with a time interval of 1 h for 24 h. The scenarios were generated in MATLAB R2021b, and the generated scenarios were reduced in the GAMS software using the CPLEX solver. To solve the MINLP optimization, the ANTIGONE framework—a deterministic, general, mixed-integer, nonlinear, global optimization framework—was utilized.

This system has three MGs, and the day-ahead predicted electric and heat demand can be found in Figure 3. The forecasted solar radiation and wind speed are also illustrated in Figure 4. The parameters of the proposed system are given in Table 1. The time of use wholesale electric price, parameters of the RES resources, and battery energy storage are taken from ref. [33]; however, the capacity of these resources has been modified. The parameters of heat storage and the efficiency of the gas boiler are taken and modified from [34] and [35], respectively.
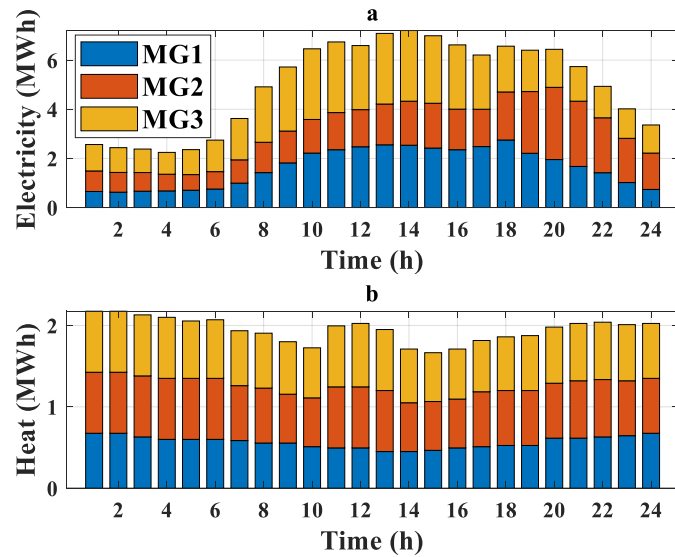


**Figure 3.** (**a**) Daily electric load profiles of the MGs; (**b**) Daily heat load profiles of the MGs.
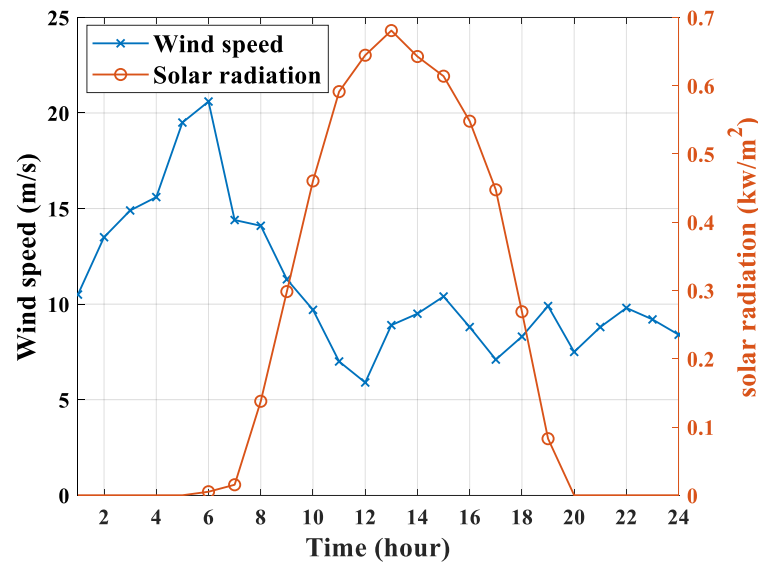


**Figure 4.** Wind speed and solar radiation.

**Table 1.** Parameters of the proposed system.

| Parameter | Value | Parameter | Value | Parameter | Value |
|---|---|---|---|---|---|
| $P_{\max}^{grid}$ | 6 MW | $P_{i,ini}^{g,CHP}$ | 0 MWh | $SoC_{i,\min}^{HS}$ | 0 MWh |
| $P_{\max}^{Gas}$ | 9 MW | $P_i^{d,CHP}$ | 1 MWh | $SoC_i^{ini,HS}$ | 0 MWh |
| $P_{i,\max}^{E}$ | 2 MW | $P_i^{u,CHP}$ | 1 MWh | $SoC_{i,\max}^{HS}$ | 0.4 MWh |
| $P_{i,\max}^{G}$ | 3 MW | $\eta_i^{GB}$ | 0.85% | $P_{i,\max}^{HS}$ | 0.2 MW |
| $\pi_{i,\min}^{E}$ | USD 30/MWh | $P_{i,\max}^{g,GB}$ | 1 MW | $P_{\max}^{DRU}$ | 10% |
| $\pi_{i,\max}^{E}$ | USD 100/MWh | $\eta^{ch,BS}$ | 95% | $P_{\max}^{DRD}$ | 10% |
| $\pi^{G}$ | USD 15/MWh | $\eta^{dch,BS}$ | 95% | $P_{STC,i}^{PV}$ | 0.4 MWh |
| $\pi^{Gas}$ | USD 20/MWh | $SoC_i^{ini,BS}$ | 0.1 MWh | $K$ | $-0.005\%/C^0$ |
| $\pi^{DR}$ | USD 3/MWh | $SoC_{i,\min}^{BS}$ | 0.1 MWh | $\Phi_i^{STC}$ | 1000 W/m$^2$ |
| $\pi^{ENS}$ | USD 400/MWh | $SoC_{i,\max}^{BS}$ | 0.9 MWh | $P_{r,i}^{WT}$ | 0.4 MWh |
| $\eta_i^{e,CHP}$ | 0.4% | $P_{i,\max}^{BS}$ | 0.25 MW | $V_{ci}$ | 4 m/s |
| $\eta_i^{h,CHP}$ | 0.35% | $\eta^{ch,HS}$ | 90% | $V_r$ | 14 m/s |
| $P_{i,\max}^{g,chp}$ | 2 MW | $\eta^{dch,HS}$ | 90% | $V_{co}$ | 25 m/s |

### 3.2. Scenario Generation and Reduction

Each uncertain parameter had seven scenarios for each time interval, so the total number of generated scenarios for four uncertain parameters was $7^4 = 2401$. This high number of scenarios was reduced to 26 scenarios using MILP scenario reduction. The PDFs of uncertain parameters were generated in MATLAB R2021b, and the generated scenarios were reduced in the GAMS software using the CPLEX solver.

### 3.3. Comparison of Different Cases

To analyze the effectiveness of the proposed system, three cases were considered as follows:

Case 1: Without ESS and DR
Case 2: With ESS and without DR
Case 3: With ESS and DR

One of the important parameters that contributes to higher MGs operational costs, according to Equation (14), is ENS. The ENS of the electrical load is illustrated in Figure 5.
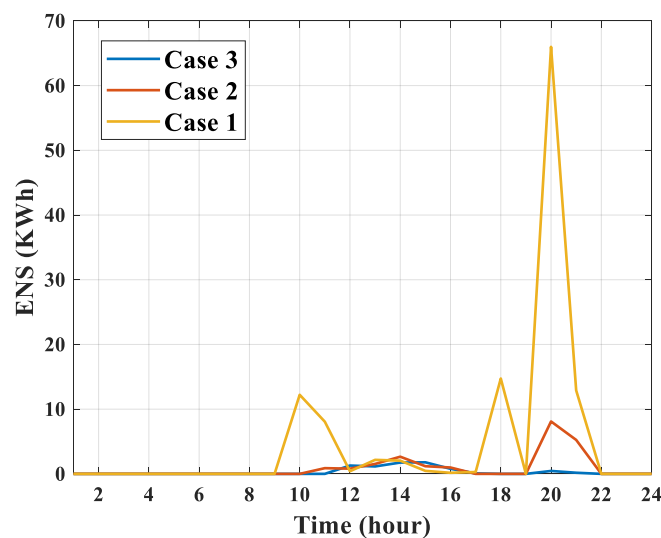


**Figure 5.** ENS of electrical load.

According to Figure 5, the ENS of the electrical load has been significantly improved by implementing both DR and ESS. The extraordinary ENS occurred on t20 in Case 1 and

had a value of 66 KWh. This value fell to 8 KWh in case 2 and almost diminished in case 3. The improvement also occurred in other hours, especially at t10 and t18. Table 2 compares the results in terms of DISCO profit, MGs cost, and ENS.

**Table 2.** Comparison of the results for different cases.

| Case | MGs Cost (USD) | DISCO Profit (USD) | ENS (MWh) |
| --- | --- | --- | --- |
| Case 1 | 9593.0917 | 4272.9564 | 0.1194 |
| Case 2 | 10,022.8378 | 4548.1967 | 0.0213 |
| Case 3 | 9474.8072 | 4431.2495 | 0.0074 |

The proposed system in Case 3 achieves a negligible ENS with 0.0074 MWh, which accounted for 0.1194 MWh in Case 1. In terms of MGs' cost, the value decreased from USD 9593.09 to USD 9474.80, representing a 1.23% decrease in the MGs' cost. Using only ESS, Case 2 increased the MGs' cost while being beneficial for DISCO with a 6% increase in profit, from USD 4272.95 to USD 4548.19. Case 3 was also in favor of DISCO since it caused a profit increase of 3.5% compared to Case 1. Overall, according to these results, the ESS was beneficial for DISCO, and the DR was beneficial for MGs, and this is mainly because both the DISCO and MGs objectives are optimized. Moreover, Case 3 was the optimal case in terms of the economics and reliability of the system, and in the following, the optimal day-ahead operation is given for Case 3.

### 3.4. Results for Case 3

Figure 6 displays the Pareto front for Case 3. The objective function of the MGs cost is minimization, and its equivalent maximization problem is max $-OF_2$. Each red point in this figure corresponds to the best solution of DISCO profit when the MGs cost is restricted by the $\varepsilon$-constraint method. The optimal solution, among all available Pareto fronts, was selected using fuzzy decision making. The weight of each objective function in the fuzzy decision-making process was set to 0.5.
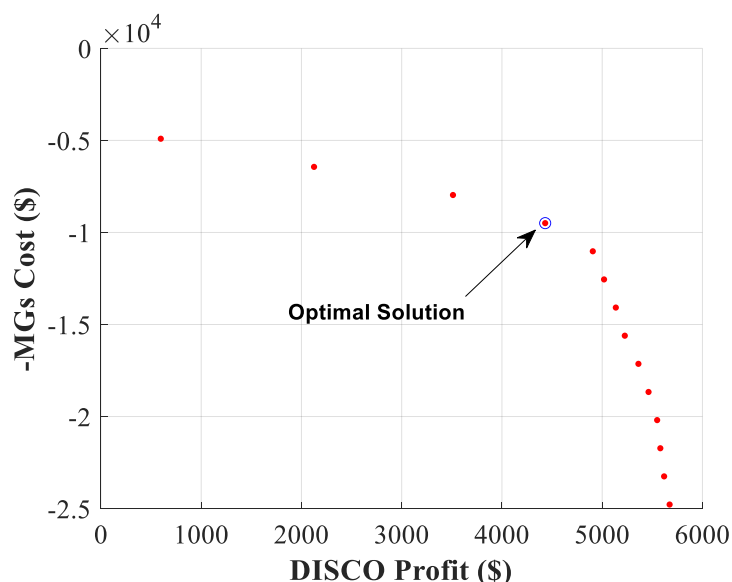


**Figure 6.** Pareto optimal front of DISCO profit and MGs Cost.

The optimal stochastic electricity management of MGs and DISCO for Case 3 is presented in Figure 7. Positive values are supply values; for example, a positive value for the grid means that the MGs or DISCO import power, and a positive value for the battery means that the battery is in a discharging state. On the other hand, negative values are considered demanded values.
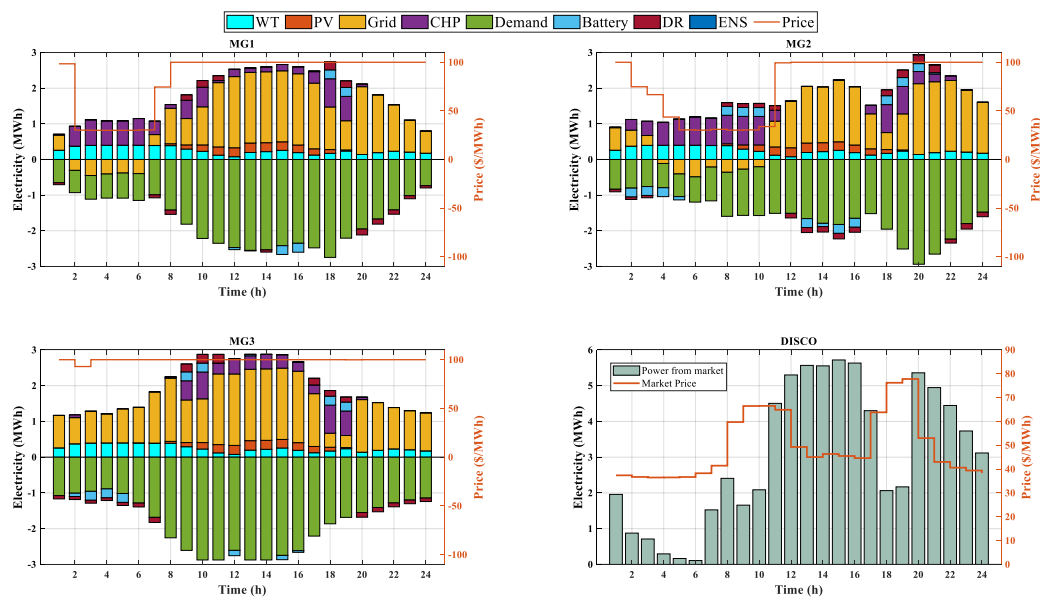
**Figure 7.** Optimal stochastic electricity management of MGs and DISCO.

In accordance with Figure 7, all MGs, apart from MG3, exported electricity in the early hours because CHP units and local renewable energy sources were able to meet the MGs' need for electricity. Any extra electricity was sold to DISCO for a price of USD 30/MWh. However, the demand for MG3 was relatively high compared to other MGs, and this MG was not able to export energy. Another effect of the increased demand was higher transactive energy prices between the MG3 and DISCO, which accounted for USD 100/MWh for nearly the entire 24 h. CHP units were mostly in operation during t1–t20 in MG1, during t2–t11 and t17–t22 in MG2, and during t9–t19 in MG3. Shift-up DR occurred during off-peak hours, while shift down occurred during on-peak hours to help MGs satisfy their demand and reduce the electric energy price. The values for ENS were so small that they are not evidently displayed in Figure 7; however, they were clearly displayed and discussed in Figure 5. Figure 7 also illustrates the power exchange between the grid and DISCO. According to this figure, DISCO imported power during all hours, and its minimum value accounted for 0.1078 MWh in t6, while its peak values were during t12–t16, and the maximum amount of power imported from the grid was at t15, with 5.7192 MWh. Although DISCO could export power to the grid, it did not happen, and the imported power to DISCO from MGs was exported to other MGs by DISCO. At t6, the entire DISCO and all the MGs were almost electrically self-satisfied. The optimal stochastic heat management of the MGs and the gas management of the MGs and DISCO are illustrated in Figure 8.

The heat demand was met through the generated heat of CHP and GB by consuming NG. GB was in operation during all hours, except for t3–t5 in MG1. Compared to the other MGs, MG3 heat demand was mostly supplied by its GB unit, especially during the early hours of scheduling, when its productions were just below 800 KWh. Since CHP produces heat and power simultaneously, the operating period of CHP units is the same as described in Figure 7. The optimal operation of heat storage can also be seen in MGs. The MGs stored energy in off-peak periods to be consumed in on-peak periods to help the system supply its heat demand optimally and reliably. As can be seen in MG2, energy storage was also able to flatten the demand profile of the heat demand by charging at t8–9 and t18–20 and discharging at t12 and t22–23. Moreover, the imported NG by MGs is illustrated in Figure 8. The stacked sum of the MGs' NG consumption is DISCO's imported NG from the grid. The imported NG by DISCO peaked at t18, with 6.05 MWh.
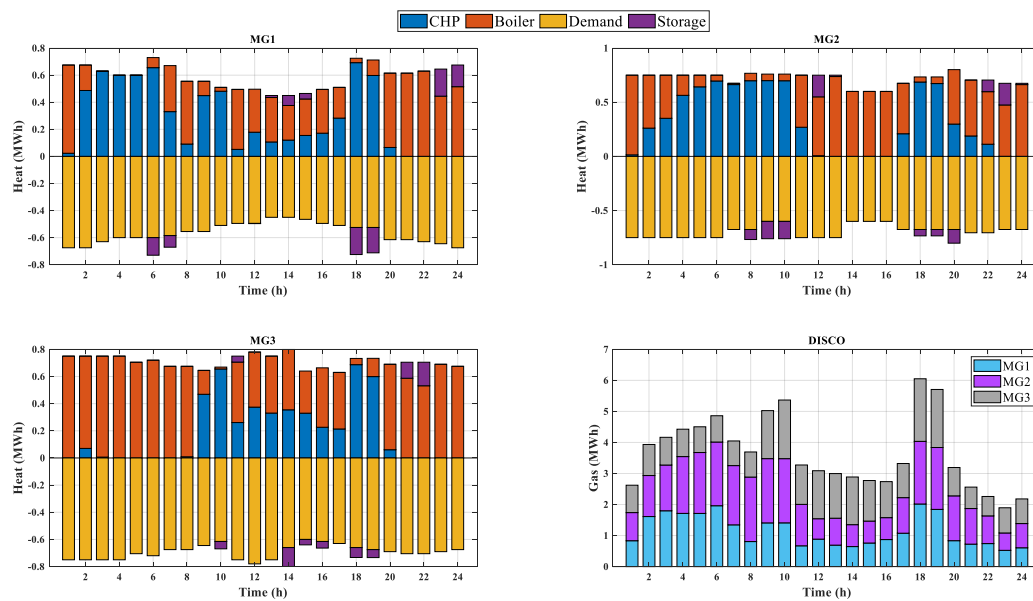
**Figure 8.** Optimal stochastic heat management of MGs and NG management of MGs and DISCO.

## 4. Conclusions

This paper presented optimal day-ahead scheduling of a multi-energy MMG system, considering the DISCO profit and MGs cost. DISCO was able to sell electrical energy and NG to MGs by purchasing these energy carriers from the grid. MGs are composed of WT, PV, CHP, GB, HS, and BS, and traded electrical energy and NG with a dynamic and fixed price. The intermittent nature of RES and its demands were addressed through scenario-based stochastic optimization. Scenarios were generated by using appropriate PDFs, and to reduce the computation complexity, the generated scenarios were reduced using MILP scenario reduction. Since the problem was multi-objective with two conflicting objective functions, the Pareto front was obtained using the $\varepsilon$-constraint method, and the best compromise of the MINLP stochastic optimization problem was selected with fuzzy decision making. According to the simulation results, the proposed strategy can achieve optimal day-ahead energy scheduling for a multi-energy MMG with great performances in both DISCO profit and MGs cost. Three cases have been investigated to understand the effect of ESS and DR on the optimal operation of the system. According to the results, implementing only ESS in the system (Case 2) increased the MGs cost, while it was beneficial for DISCO, with a 6% increase in profit, so this case was not interesting for MGs. On the other hand, presenting both ESS and DR, Case 3, caused the MGs cost reduction to be 1.23% lower and the DISCO profit increase to be 3.5% higher. Furthermore, the reliability of the system improved, with the ENS of the system reducing from 0.1194 MWh to 0.0074 MWh. Further studies will investigate other approaches to solving multi-objective optimization in microgrids, such as converting multi-stage optimization to single-stage optimization. In addition, it is suggested to consider more reliability indices in the proposed system and to add more flexibility to the system.

**Author Contributions:** Conceptualization, S.R.S. and A.S.; methodology, M.F.; software, S.R.S.; validation, S.N.R., A.Q., and M.Y.; formal analysis, M.F.; investigation, A.S.; resources, A.Q.; data curation, S.R.S.; writing—original draft preparation, S.R.S. and A.S.; writing—review and editing, M.F. and A.Q.; visualization, S.N.R. and M.Y.; supervision, A.S.; project administration, M.F. All authors have read and agreed to the published version of the manuscript.

**Data Availability Statement:** Not applicable.

## Nomenclature

**Indices**

| | |
|---|---|
| $t$ | Index of time |
| $i$ | Index of microgrids |
| $s$ | Index of scenarios |
| $n$ | Index of objective functions |

**Parameters**

| | |
|---|---|
| $P^{WT}_{t,i,s}$ | Output power of WTs at time t and scenario s [MWh] |
| $P^{PV}_{t,i,s}$ | Output power of PVs at time t and scenario s [MWh] |
| $P^{WT}_{i,r}$ | Rated power of WTs [MW] |
| $v_{t,s}$ | Wind speed at time t and scenario s [m/s] |
| $V_{ci}, V_{co}, V_r$ | Cut in, cut out and rated speed of WT |
| $P^{STC}_{PV,i}$ | PV power output at STC |
| $\Phi_{t,s}$ | Irradiance at time t and scenario s [p.u] |
| $\Phi^{STC}_i$ | Irradiance at STC condition [p.u] |
| $K$ | PV temperature coefficient of power |
| $T_{a,t}$ | Ambient temperature at time t |
| $\pi^{Grid}_t$ | Grid price for electricity at time t [USD/MWh] |
| $\pi^{Gas}$ | Grid price for NG |
| $\pi^E_{i,max}, \pi^E_{i,min}$ | Maximum/Minimum price of energy exchange between MGs and DISCO |
| $P^{Grid}_{max}$ | Maximum electricity imported from grid |
| $P^{Gas}_{max}$ | Maximum NG imported from grid |
| $k, c$ | Shape/scale index |
| $\delta, \mu$ | Standard deviation/mean value |
| $\alpha, \beta$ | Shape parameters |
| $P^{BS}_{max}, P^{HS}_{max}$ | Maximum charging & discharging of battery/heat storage [MW] |
| $SoC^{BS}_{i,ini}, SoC^{HS}_{i,ini}$ | Initial energy storage of battery/heat storage [MWh] |
| $SoC^{BS}_{i,max}, SoC^{BS}_{i,min}$ | Maximum/Minimum SoC of battery [MWh] |
| $SoC^{HS}_{i,max}, SoC^{HS}_{i,min}$ | Maximum/Minimum SoC of heat storage [MWh] |
| $P^{DRU}_{i,max}, P^{DRD}_{i,max}$ | maximum shift UP/DOWN power of DR |
| $\eta^{ch,BS}, \eta^{dch,BS}$ | Charging & discharging efficiency of battery [%] |

| | |
|---|---|
| $\eta^{e,CHP}_i, \eta^{h,CHP}_i$ | Electricity/heat efficiency of CHP unit [%] |
| $P^{g,GB}_{i,max}$ | Maximum capacity of GB unit [MW] |
| $\eta^{GB}_i$ | Heat efficiency of GB unit [%] |

**Variables**

| | |
|---|---|
| $Z^{ch,BS}_{t,i}, Z^{dch,BS}_{t,i}$ | Binary variable for battery charging and discharging power |
| $Z^{ch,HS}_{t,i}, Z^{dch,HS}_{t,i}$ | Binary variable for SC charging and discharging power |
| $Z^{DRU}_{t,i}, Z^{DRD}_{t,i}$ | Binary variable for shift UP/DOWN of DR |
| $P^{e,CHP}_{t,i,s}, P^{h,CHP}_{t,i,s}$ | Electricity/heat production of CHP unit [MWh] |
| $P^{g,CHP}_{t,i,s}$ | Consumed NG by CHP unit [MWh] |
| $P^{h,GB}_{t,i,s}, P^{g,GB}_{t,i,s}$ | Heat production/NG consumption of GB unit [MWh] |
| $\pi^E_{t,i,s}$ | Price of power exchange between DISCO and MG i [USD/MWh] |
| $P^E_{t,i,s}$ | Power exchange between DISCO and MG i [MW] |
| $P^G_{t,i,s}$ | NG imported from DISCO by MG i [MW] |
| $P^{Grid}_{t,s}$ | Power purchased from wholesale grid [MW] |
| $P^{Gas}_{t,s}$ | NG purchased from wholesale grid [MW] |
| $P^{ch,BS}_{t,i}, P^{dch,BS}_{t,i}$ | Charging and discharging power of battery [MWh] |
| $P^{ch,HS}_{t,i}, P^{dch,HS}_{t,i,s}$ | Charging/discharging power of heat storage [MWh] |
| $SoC^{BS}_{t,i,s}, SoC^{HS}_{t,i,s}$ | Stat of charge of battery/heat storage [MWh] |
| $P^{ENS}_{t,i,s}$ | ENS of load |
| $P^{DRU}_{t,i}, P^{DRD}_{t,i}$ | shift UP/DOWN power of DR |

**Acronym**

| | |
|---|---|
| MMG | Multi-microgrids |
| DISCO | Distribution company |
| RES | Renewable energy source |
| WT | Wind turbine |
| PV | Photovoltaic |
| B | Battery |
| PDF | Probability density function |
| MILP | Mixed-integer linear programming |

| | | | |
|---|---|---|---|
| $\eta^{ch,HS}, \eta^{dch,HS}$ | Charging & discharging efficiency of heat storage [%] | $MINLP$ | Mixed-integer nonlinear programming |
| $\pi^{DR}, \pi^{ENS}$ | Cost of DR/ENS [USD/MW h] | $MG$ | Microgrid |
| $P_{i,\max}^{E}$ | Maximum exchange power between DISCO and MG i [MW] | $DR$ | Demand response |
| $P_{i,\max}^{G}$ | Maximum imported NG from DISCO by MG i [MW] | $SoC$ | State of charge |
| $\rho_{t,s}$ | Probability for scenario s at time t | $STC$ | Standard testing condition |
| $P_{i,\max}^{g,CHP}$ | Maximum capacity of CHP unit [MW] | $NG$ | Natural gas |
| $P_{t,i}^{u,CHP}, P_{t,i}^{d,CHP}$ | Ramp up/down limit of CHP unit [MW] | $CHP$ | Combined heat and power |
| | | $ENS$ | Energy not supplied |

## References

1. Cai, Y.; Lu, Z.; Pan, Y.; He, L.; Guo, X.; Zhang, J. Optimal scheduling of a hybrid AC/DC multi-energy microgrid considering uncertainties and Stackelberg game-based integrated demand response. *Int. J. Electr. Power Energy Syst.* **2022**, *142*, 108341. [CrossRef]
2. Wang, J.; Li, K.-J.; Liang, Y.; Javid, Z. Optimization of Multi-Energy Microgrid Operation in the Presence of PV, Heterogeneous Energy Storage and Integrated Demand Response. *Appl. Sci.* **2021**, *11*, 1005. [CrossRef]
3. Li, Z.; Xu, Y.; Feng, X.; Wu, Q. Optimal Stochastic Deployment of Heterogeneous Energy Storage in a Residential Multienergy Microgrid With Demand-Side Management. *IEEE Trans. Ind. Inform.* **2021**, *17*, 991–1004. [CrossRef]
4. Karimi, H.; Jadid, S.; Makui, A. Stochastic energy scheduling of multi-microgrid systems considering independence performance index and energy storage systems. *J. Energy Storage* **2021**, *33*, 102083. [CrossRef]
5. Vera, E.G.; Cañizares, C.A.; Pirnia, M.; Guedes, T.P.; Melo, J.D. Two-Stage Stochastic Optimization Model for Multi-Microgrid Planning. *IEEE Trans. Smart Grid* **2022**. [CrossRef]
6. Bashardoust, A.; Farrokhifar, M.; Fard, A.Y.; Safari, A.; Mokhtarpour, E. Optimum Network Reconfiguration to Improve Power Quality and Reliability in Distribution System. *Int. J. Grid Distrib. Comput.* **2016**, *9*, 101–110. [CrossRef]
7. Iqbal, S.; Mehran, K. A Day-Ahead Energy Management for Multi MicroGrid System to Optimize the Energy Storage Charge and Grid Dependency—A Comparative Analysis. *Energies* **2022**, *15*, 4062. [CrossRef]
8. Ranjbarzadeh, H.; Tafreshi, S.M.; Ali, M.H.; Kouzani, A.Z.; Khoo, S. A Probabilistic Model for Minimization of Solar Energy Operation Costs as Well as $CO_2$ Emissions in a Multi-Carrier Microgrid (MCMG). *Energies* **2022**, *15*, 3088. [CrossRef]
9. Farrokhifar, M.; Nie, Y.; Pozo, D. Energy systems planning: A survey on models for integrated power and natural gas networks coordination. *Appl. Energy* **2020**, *262*, 114567. [CrossRef]
10. Li, Y.; Wang, K.; Gao, B.; Zhang, B.; Liu, X.; Chen, C. Interval optimization based operational strategy of integrated energy system under renewable energy resources and loads uncertainties. *Int. J. Energy Res.* **2021**, *45*, 3142–3156. [CrossRef]
11. Hussain, A.; Bui, V.-H.; Kim, H.-M. Robust Optimization-Based Scheduling of Multi-Microgrids Considering Uncertainties. *Energies* **2016**, *9*, 278. [CrossRef]
12. Hou, J.; Yu, W.; Xu, Z.; Ge, Q.; Li, Z.; Meng, Y. Multi-time scale optimization scheduling of microgrid considering source and load uncertainty. *Electr. Power Syst. Res.* **2023**, *216*, 109037. [CrossRef]
13. Pezhmani, Y.; Oskouei, M.Z.; Rezaei, N.; Mehrjerdi, H. A centralized stochastic optimal dispatching strategy of networked multi-carrier microgrids considering transactive energy and integrated demand response: Application to water–energy nexus. *Sustain. Energy Grids Netw.* **2022**, *31*, 100751. [CrossRef]
14. Farrokhifar, M.; Aghdam, F.H.; Alahyari, A.; Monavari, A.; Safari, A. Optimal energy management and sizing of renewable energy and battery systems in residential sectors via a stochastic MILP model. *Electr. Power Syst. Res.* **2020**, *187*, 106483. [CrossRef]
15. Safari, A.; Farrokhifar, M.; Shahsavari, H.; Hosseinnezhad, V. Stochastic planning of integrated power and natural gas networks with simplified system frequency constraints. *Int. J. Electr. Power Energy Syst.* **2021**, *132*, 107144. [CrossRef]
16. Pippia, T.; Lago, J.; De Coninck, R.; De Schutter, B. Scenario-based nonlinear model predictive control for building heating systems. *Energy Build.* **2021**, *247*, 111108. [CrossRef]
17. Carli, R.; Cavone, G.; Pippia, T.; Schutter, B.D.; Dotoli, M. Robust Optimal Control for Demand Side Management of Multi-Carrier Microgrids. *IEEE Trans. Autom. Sci. Eng.* **2022**, *19*, 1338–1351. [CrossRef]
18. Gunantara, N. A review of multi-objective optimization: Methods and its applications. *Cogent Eng.* **2018**, *5*, 1502242. [CrossRef]
19. Baringo, L.; Conejo, A.J. Correlated wind-power production and electric load scenarios for investment decisions. *Appl. Energy* **2013**, *101*, 475–482. [CrossRef]
20. Rastegar, M.; Fotuhi-Firuzabad, M.; Lehtonen, M. Home load management in a residential energy hub. *Electr. Power Syst. Res.* **2015**, *119*, 322–328. [CrossRef]
21. Latifi, H.; Farrokhifar, M.; Safari, A.; Pournasir, S. Optimal sizing of combined heat and power generation units using of MPSO in the Besat Industrial Zone. *Int. J. Energy Stat.* **2016**, *4*, 1650002. [CrossRef]
22. Lu, Z.; Gao, Y.; Xu, C.; Li, Y. Configuration optimization of an off-grid multi-energy microgrid based on modified NSGA-II and order relation-TODIM considering uncertainties of renewable energy and load. *J. Clean. Prod.* **2023**, *383*, 135312. [CrossRef]
23. Ghiasi, M.; Niknam, T.; Dehghani, M.; Siano, P.; Alhelou, H.H.; Al-Hinai, A. Optimal Multi-Operation Energy Management in Smart Microgrids in the Presence of RESs Based on Multi-Objective Improved DE Algorithm: Cost-Emission Based Optimization. *Appl. Sci.* **2021**, *11*, 3661. [CrossRef]
24. Ullah, K.; Hafeez, G.; Khan, I.; Jan, S.; Javaid, N. A multi-objective energy optimization in smart grid with high penetration of renewable energy sources. *Appl. Energy* **2021**, *299*, 117104. [CrossRef]
25. Sedighizadeh, M.; Esmaili, M.; Mohammadkhani, N. Stochastic multi-objective energy management in residential microgrids with combined cooling, heating, and power units considering battery energy storage systems and plug-in hybrid electric vehicles. *J. Clean. Prod.* **2018**, *195*, 301–317. [CrossRef]
26. Hadayeghparast, S.; Farsangi, A.S.; Shayanfar, H.; Karimipour, H. Stochastic Multi-objective Economic/Emission Energy Management of a Microgrid in Presence of Combined Heat and Power Systems. In Proceedings of the 2019 IEEE/IAS 55th Industrial and Commercial Power Systems Technical Conference (I&CPS), Calgary, AB, Canada, 5–8 May 2019; pp. 1–9. [CrossRef]
27. Shen, Y.; Hu, W.; Liu, M.; Yang, F.; Kong, X. Energy storage optimization method for microgrid considering multi-energy coupling demand response. *J. Energy Storage* **2022**, *45*, 103521. [CrossRef]

28. Gimelli, A.; Mottola, F.; Muccillo, M.; Proto, D.; Amoresano, A.; Andreotti, A.; Langella, G. Optimal configuration of modular cogeneration plants integrated by a battery energy storage system providing peak shaving service. *Appl. Energy* **2019**, *242*, 974–993. [CrossRef]

29. Farsangi, A.S.; Hadayeghparast, S.; Mehdinejad, M.; Shayanfar, H. A novel stochastic energy management of a microgrid with various types of distributed energy resources in presence of demand response programs. *Energy* **2018**, *160*, 257–274. [CrossRef]

30. Karuppiah, R.; Martín, M.; Grossmann, I.E. A simple heuristic for reducing the number of scenarios in two-stage stochastic programming. *Comput. Chem. Eng.* **2010**, *34*, 1246–1255. [CrossRef]

31. Soroudi, A. Simple Examples in GAMS. In *Power System Optimization Modeling in GAMS*; Soroudi, A., Ed.; Springer International Publishing: Cham, Switzerland, 2017; pp. 33–63.

32. Rabiee, A.; Soroudi, A.; Mohammadi-ivatloo, B.; Parniani, M. Corrective Voltage Control Scheme Considering Demand Response and Stochastic Wind Power. *IEEE Trans. Power Syst.* **2014**, *29*, 2965–2973. [CrossRef]

33. Bahramara, S.; Moghaddam, M.P.; Haghifam, M.R. Modelling hierarchical decision making framework for operation of active distribution grids. *IET Gener. Transm. Distrib.* **2015**, *9*, 2555–2564. [CrossRef]

34. Nikmehr, N. Distributed robust operational optimization of networked microgrids embedded interconnected energy hubs. *Energy* **2020**, *199*, 117440. [CrossRef]

35. Shams, M.H.; Shahabi, M.; Khodayar, M.E. Stochastic day-ahead scheduling of multiple energy Carrier microgrids with demand response. *Energy* **2018**, *155*, 326–338. [CrossRef]